https://doi.org/10.5194/egusphere-2024-1530
Preprint. Discussion started: 21 June 2024

Characterizing Spatial Structures of Field-Scale Snowpack using Unpiloted Aerial System (UAS) Lidar and SfM Photogrammetry

Eunsang Cho[1†], Megan Verfaillie[2,3†], Jennifer M. Jacobs[2,3], Adam G. Hunsaker[3], Franklin B. Sullivan[3], Michael Palace[3,4], Cameron Wagner[2,3*]

[1]Ingram School of Engineering, Texas State University, San Marcos, USA
[2]Department of Civil and Environmental Engineering, University of New Hampshire, Durham, NH, USA
[3]Earth Systems Research Center, Institute for the Study of Earth, Oceans, and Space, University of New Hampshire, Durham, NH, USA
[4]Department of Earth Sciences, University of New Hampshire, Durham, NH, USA
[*]Present address: U.S. Army Cold Regions Research and Engineering Laboratory, Hanover, NH, USA

[†]These authors contributed equally to this work.

Correspondence to: Eunsang Cho (eunsang.cho@txstate.edu)

Abstract. Uncrewed Aerial Systems (UAS) lidar and structure-from-motion (SfM) photogrammetry have emerged as viable methods to map high-resolution snow depths (~1 m). These technologies enable a better understanding of snowpack spatial structure and its evolution over time, advancing hydrologic and ecological applications. In this study, a series of UAS lidar/SfM snow depth maps were collected during the 2020/21 winter season in Durham, New Hampshire, USA with three objectives: (1) quantifying UAS lidar/SfM snow depth retrieval performance using multiple in-situ measurement techniques (magnaprobe and field cameras), (2) conducting a quantitative comparison of lidar and SfM snow depths (< 35 cm) throughout the winter, and (3) better understanding the spatial structure of snow depth and its relationship with terrain features. The UAS surveys were conducted over approximately 0.35 km^2 including both open fields and a mixed forest. In the field, lidar had a lower error than SfM compared to in-situ observations with a Mean Absolute Error (MAE) of 3.0 cm for lidar and 5.0 - 14.3 cm for SfM. In the forest, SfM greatly overestimated snow depths compared to lidar (lidar MAE = 2.7 - 7.3 cm, SfM MAE = 32.0 - 44.7 cm). Even though snow depth differences between the magnaprobe and field cameras were found, they had only a modest impact on the UAS snow depth validation. Using the concept of temporal stability, we found that the spatial structure of snow depth captured by lidar was generally consistent throughout the period indicating a strong influence from static land characteristics. Considering all areas (forest and fields), the spatial structure of snow depth was primarily influenced by vegetation type (e.g., fields, deciduous, and coniferous forests). Within the field, the spatial structure was primarily correlated with slope and forest canopy shadowing effects.

1 Introduction

Spatial patterns of hydrologic state variables and fluxes including soil moisture, snow, interception, precipitation, and evapotranspiration reflect underlying static physical conditions and dynamic forcing from weather events. These patterns serve

https://doi.org/10.5194/egusphere-2024-1530
Preprint. Discussion started: 21 June 2024

a variety of purposes including downscaling remotely sensed or model output, upscaling in situ observations, assimilation to update model simulations, and as proxies or analogues for similar hydrologic units. They can also provide insight into underlying landscape features, biogeochemical processes, and habitat viability.

Snowpacks play a crucial role in hydrologic, climatic, and ecological processes at various scales (Barnett et al., 2005). Snowpack structure and its temporal evolution are important to determine snowmelt runoff, infiltration, and groundwater recharge (Carroll et al., 2019; Harpold et al., 2015; Maurer and Bowling, 2014) as well as energy partitioning processes (Lawrence and Slater, 2010; Stieglitz et al., 2001; Sturm et al., 2017). Snowpack also exerts a strong control on snow-soil interactions because the insulating capacities of snowpack affect the underlying soil freeze-thaw state influencing soil respiration, nutrient retention, and carbon dynamics (Anderton et al., 2002; Schlogl et al. 2018; Cho et al., 2021; Monson et al., 2006; Sorensen et al., 2018; Reinmann and Templer, 2018; Wilson et al., 2020; Yi et al., 2015).

The spatial variability of a snowpack is a function of static and dynamic variables over a range of spatial scales (Clark et al., 2011; Grayson et al., 2002; Mott and Lehning, 2011; Trujillo et al., 2007). Over time, spatial patterns may evolve and change, but many hydrologic patterns persist until they are modified by weather conditions. Spatial snowpack patterns and their consistency, or repeatability, play a crucial role in various applications, including operational snowmelt predictions, the downscaling of remotely sensed or model outputs, the integration of in situ observations through upscaling, the assimilation of data to enhance model simulations, and the utilization of snowpack characteristics as proxies or analogs for similar hydrological units (Pflug and Lundquist, 2020; Cho et al., 2023). They can also provide insight into underlying landscape features, biogeochemical processes, and wildlife habitats (Boelman et al., 2019; Pflug et al., 2023).

Traditionally, field or local-scale snow features are captured through in situ observations and field campaigns (Clark et al., 2011; Trujillo et al., 2007), whereas regional or continental-scale patterns are typically observed using airborne and satellite remote sensing techniques (Lievens et al., 2022; Painter et al., 2016; Derksen et al., 2005). Airborne and satellite remote sensing methods have provided the ability to collect snowpack data over a large spatial extent, thus expanding the understanding of snow distribution (Cho et al., 2019; Lievens et al., 2022; Painter et al., 2016; Tsang et al., 2021). However, the capture of small-scale snow patterns, discerned through field campaigns or less frequent, routine operational collections, is often hindered by challenges such as weather conditions and site accessibility which can lead to infrequent sampling during the winter season.

Uncrewed Aerial Systems (UASs) have been used to provide spatially continuous, opportunistic snow-covered area and snow depth observations at scales between in situ and airborne and satellite remote sensing (Bühler et al., 2016; De Michele et al., 2016; Harder et al., 2016; 2020; Meyer et al., 2022; Revuelto et al., 2021). UAS-based remote sensing enables the acquisition of data at finer spatial resolutions, reaching scales as precise as centimeters for a designated area. UAS platforms also offer a cost-effective alternative to aerial surveys, facilitating routine monitoring of snow conditions (Gaffey et al., 2020). Hence, the capabilities of UAS platforms equipped with diverse sensors allow for the observation of field-scale physical interactions between snowpacks and land/soil characteristics (Cho et al., 2021).

https://doi.org/10.5194/egusphere-2024-1530
Preprint. Discussion started: 21 June 2024

UAS lidar and Structure-from-Motion (SfM) photogrammetry have emerged as viable methods for mapping high-resolution snow depths (~1 m), enabling a better understanding of snowpack spatial structure and its evolution over time at the field scale (Feng et al., 2023; Harder et al., 2019; Jacobs et al., 2021; Koutantou., 2022). As the use of UAS-based high-resolution snow depth mapping becomes more prevalent, there is a growing need for a comprehensive understanding of their strengths and weaknesses for capturing snowpack evolution throughout the entire snow period for various landscape features (e.g., forest and fields). However, investigating these transition periods poses challenges, primarily due to the snow becoming increasingly shallow and patchy, eventually revealing bare ground. Despite these challenges, these transition periods hold significant hydrological, ecological, and energy implications (Harrison et al., 2021; Harpold et al., 2017; Grogan et al., 2020).

This study aims to achieve three main objectives using a series of UAS lidar/SfM snow depth maps over a mixed-use temperate forest landscape: (1) quantify UAS snow depth retrieval performance by comparing it with multiple in-situ measurement techniques, (2) conduct a quantitative comparison of lidar and SfM snow depths (< 35 cm) throughout the snow period, and (3) gain a better understanding of the spatial structure of snow depth, its stability over time, and its relationship with multiple physical terrain features. This paper is organized as follows: Section 2 provides an overview of the study area, including its land characteristics. Section 3 describes the datasets utilized in the study, including UAS lidar, SfM photogrammetry, field observations, and the methods employed, such as the relative difference concept. Section 4 presents the results, with subsections detailing comparisons between UAS snow depth and in-situ measurements (4.1), as well as comparisons between lidar and SfM snow depth (4.2). Additionally, spatial structures and temporal changes in snow depth, along with relevant physical variables characterizing those snow patterns, are discussed in Sections 4.3 and 4.4. Section 5 discusses new insights derived from the comparison results and spatial structures of snow depth, along with the limitations of this study and future perspectives. Finally, conclusions are drawn in Section 6.

2 Study area

This study was conducted at the University of New Hampshire Thompson Farm Research Station in southeast New Hampshire, United States (N 43.10892°, W 70.94853°, 35 m above sea level), which was chosen for its mixed hardwood forest and open field land covers (Perron et al. 2004; Burakowski et al., 2015; Jacobs et al., 2021) that are characteristic of the region (Error! Reference source not found.). Thompson Farm has an area of 0.83 km^2 and little topographic relief (18 to 36 m ASL) (Perron et al., 2004). The agricultural fields are actively managed for pasture grass with unmown grass. The deciduous, mixed, and coniferous forest is composed primarily of white pine (Pinus strobus), northern red oak (Quercus rubra), red maple (Acer rubrum), shagbark hickory (Carya ovata), and white oak (Quercus alba). The forest soils are classified as Hollis/Charlton very stony-fine sandy loam and well-drained; field soils are characterized as Scantic silt-loam and poorly drained (Perron et al. 2004). There are two logging access roads running north-south through the pasture and western forest section. The winter climate at Thompson Farm is characterized by cold, maritime winter climate with a mean winter air temperature of -3.0°C, annual snowfall of 114 cm, and three weeks to over three months of days having snow cover (Burakowski and Hamilton,

https://doi.org/10.5194/egusphere-2024-1530
Preprint. Discussion started: 21 June 2024

2020). Average wind speed was 1.41 m/s for the study period. Snow depth can range from a trace up to 94 cm and typical snow density ranges from 100 to 400 kg/m^3 (Burakowski and Hamilton, 2020).

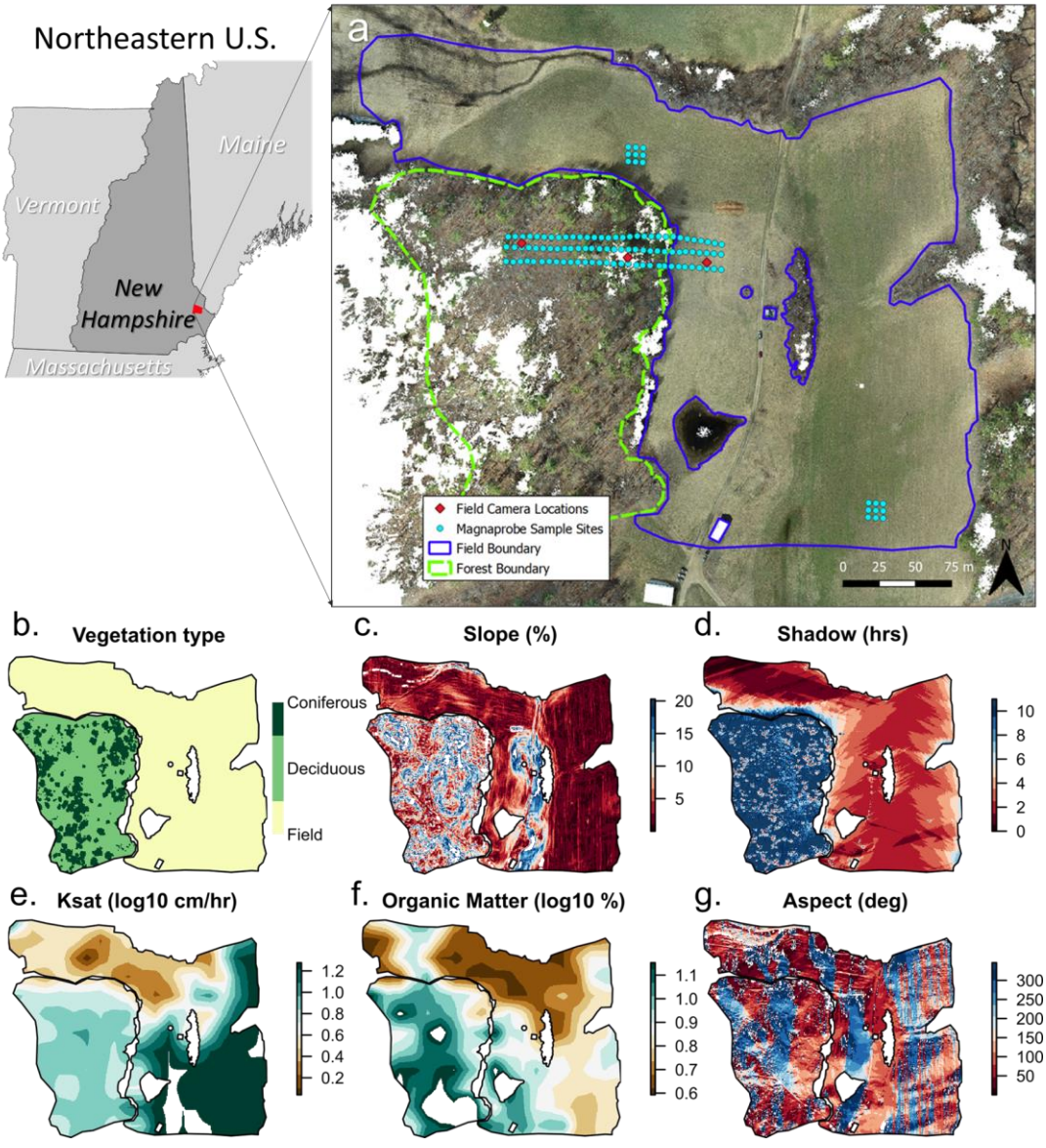

Figure 1. Summary of Thompson Farm survey area located in Durham, NH, USA. (a) In-situ sample sites and field and forest boundaries are overlain on the snow-off imagery. Maps of (b) vegetation type, (c) slope, (d) shadow hour, (e) soil hydraulic conductivity (K_{sat}), (f) organic matter, and (g) aspect are shown for both the field and forest areas.

https://doi.org/10.5194/egusphere-2024-1530
Preprint. Discussion started: 21 June 2024

3 Datasets and methods

A series of UAS lidar surveys, UAS SfM photogrammetry surveys, and in-situ sample campaigns were conducted at Thompson Farm during the winter 2020-2021. Eight snow-on campaigns were conducted between February 10th and March 11th, 2021 during which UAS lidar, UAS SfM photogrammetry and in-situ data were collected (**Table 1**). The UAS snow-on surveys were conducted prior to in-situ sampling on each of the campaign dates. A snow-off baseline survey was conducted on April 2nd, 2021 following snowmelt.

Table 1. Number of 1x1 meter grid cells sampled by land cover type for each snow-on UAV flight over the field campaign period in 2021. Each grid cell was comprised of nine Magnaprobe snow depth measurements and one snow tube SWE measurement.

Date	Number of samples (Field)	Number of samples (Coniferous)	Number of samples (Deciduous)	Number of samples (Mixed)
Feb 4th	30	9	9	9
Feb 10th	9	2	1	1
Feb 20th	9	4	1	1
Feb 23th	9	4	1	1
Feb 24th	30	9	9	9
Feb 28th	9	4	1	1
Mar 3rd	9	3	1	1
Mar 7th	9	4	1	1

3.1 UAS LiDAR and SfM photogrammetry

The lidar sensor payload consisted of the Velodyne VLP-16 laser scanner, and the Applanix APX-15 Inertial Navigation System (INS; GNSS+IMU). The VLP-16 is a lightweight (~830 grams) low power (~8W) sensor, which makes it ideal for UAS deployment. The sensor incorporates 16 rotating IR lasers that are arranged and oriented on the payload to provide a 30° along-track field of view with a cross-track field of view limited only by the range of the sensor (approximately 100 m). At an altitude of 65 m, the range of the sensor produces an effective cross-track field of view of approximately 98°. Each laser operates at a wavelength of 903 nm.

For these acquisition missions, the VLP-16 was hard-mounted to a DJI Matrice 600 to maintain constant lever arm offsets between the inertial navigation system (INS) GNSS antenna, the lidar sensor, and the INS board. As opposed to a gimbal mounted system, this hard-mounted configuration achieves a more tightly coupled system, resulting in improved point cloud geolocation accuracy. The lidar sensor was set to dual-return mode to improve ground detection in the forested areas of our field site. We flew the system at an altitude of 65 m with a flight speed of 3 m/s and ~40 m spacing between flight lines. Flights produced between a total of ~70-140 million returns per mission, depending on site ground conditions.

https://doi.org/10.5194/egusphere-2024-1530
Preprint. Discussion started: 21 June 2024

Lidar observations were georeferenced using position and attitude measurements acquired with the Applanix APX-15 Inertial Navigation System (INS). The INS produced 2–5-cm positional, 0.025-degree roll and pitch, and 0.08-degree true heading uncertainties following post-processing. Post-processing of INS data was performed using POSPac UAV (v. 8.2.1, Applanix Corporation 2018), correcting differentially against a permanent Continuously Operating Reference Station (CORS) at the University of New Hampshire in Durham, NH (NHUN). Position and attitude data were output as a Smoothed Best Estimate of Trajectory (SBET), then time synchronized with lidar returns to produce a georeferenced point cloud using LidarTools (v. 3.1.4, Headwall Photonics, Inc.).

Three-dimensional point clouds were processed using a progressive morphological filter (PMF) within the R programing language package 'lidR' to identify ground returns. For ground classification, point clouds were chunked into 100-m square tiles with a 15-m buffer on all sides using catalogue options in lidR to ensure returns near tile edges were classified. The PMF was parameterized using a set of window sizes of 1, 3, 5, and 9 m, and elevation thresholds of 0.2, 1.5, 3, and 7 m, which were determined by varying value sets and assessing digital terrain models (DTMs) to determine the parameter sets that produced a visually smooth surface over a dense grid (Muir et al. 2017). Following ground classification for each tile, returns within the 15-m tile buffers were removed, and all resulting 100-m square ground classified tiles were merged. The result of the PMF is that non-ground returns (i.e., trees, shrubs, and noise) were filtered out of the point cloud data sets, so that only returns from ground surfaces remained. The two data sets, non-ground returns and ground returns from the original point clouds, were coded according to LAS specifications and merged. Lidar snow depths were calculated as the difference between the ground classified snow-on and snow-off elevations within each pixel. For comparison to in situ observations, the ground returns were extracted for the 1 x 1 m square sampling sites, corresponding to the alignment and orientation of the respective PVC grids. The lidar snow depth was calculated as the difference between the mean snow-on and mean snow-off elevations within each sampling grid.

Photogrammetry bare-earth and snow-on elevation models were constructed from UAS-borne optical imagery. RGB images were collected with the DJI Phantom 4 Real Time Kinematic (RTK) UAS platform equipped with a 20-megapixel CMOS sensor. The RTK system integrates a static base station that relays GNSS corrections to the UAS, enabling sub-centimeter accuracy of image geotags. To ensure photogrammetry snow depth products align correctly with the UAS lidar products, the RTK base-station was placed over a monument with known coordinates which were entered into the DJI flight app. Flights were conducted at an altitude of 65 m AGL and a flight speed of 8 m/s. The shutter triggering interval was set to achieve a forward overlap of 80% between image pairs and the flight lines were spaced to achieve 80% side overlap. Three Ground Control Points (GCPs) were placed within the AOI to verify the accuracy of the photogrammetry products. The GCPs were surveyed in using base/rover RTK equipment with sub-centimeter accuracy.

The acquired image datasets were processed through the basic photogrammetry workflow using Agisoft Metashape (version 1.8.4). Sparse clouds were constructed using the default key point and tie point limits of 40,000 and 4,000, respectively. Points with high errors within the sparse clouds were then removed using the gradual selection tool. This included points exceeding the following thresholds; reprojection error > 0.5, reconstruction uncertainty > 50, and projection accuracy >5. The camera

https://doi.org/10.5194/egusphere-2024-1530
Preprint. Discussion started: 21 June 2024

intrinsic/extrinsic parameters were optimized following the removal of the poorly localized points. Dense clouds were then made with the quality setting set to high and depth filtering set to moderate. Ground returns were classified using the ground classification tool within Metahape. A first pass at establishing a ground surface is done by triangulating the lowest point elevation within 50-m grid cells. The default thresholds for maximum distance and angle (1 m and 15 degrees respectively) of all points relative to the triangulated surface were used to determine which points are part of the ground surface. Finally, digital elevation models (DEMs) were made based on the ground classified points within the dense clouds. Snow depth products were derived following the same procedure as the lidar.

3.2 Field observations

In-situ snow depth sampling was conducted in the field and forest using two methods: a Snow-Hydro LLC magnaprobe and three Moultrie Wingscapes Birdcam Pro Field Cameras. The magnaprobe sampling was conducted along three parallel transects (39 points) and at two rectangular areas (18 points). The three transects were each approximately 145 m long and were laid out from east to west and separated by approximately 10 m, north to south (**Figure 1**). From east to west, each transect started in the open field area, then transitioned to the coniferous, then mixed, and finally, deciduous forested areas. The two rectangular areas were located in the open field; one in the northwest portion and the other in the southeast. At each point, nine measurements were taken within 1 m x 1 m grid cells. It is worth noting that sampling was not conducted for every flight. Full sampling occurred on February 4th and 24th, while selective sampling was conducted on the remaining dates (**Table 1**). All sampling locations were geolocated using a Trimble© Geo7X GNSS Positioning Unit and Zephyr™ ^{antenna} with an estimated horizontal uncertainty of 2.51 cm (standard deviation 0.95 cm) in the field and 4.17 cm (standard deviation 4.60 cm) in the forest after differential correction.

Field camera snow depths were acquired following the method used in NASA's 2020 SnowEx field campaign in Grand Mesa, CO (personal communication, 16th November 2023). The three cameras were placed in each land cover type; one in the open field, one in the coniferous forest, and one in the deciduous forest. Each camera was mounted approximately 0.85 m above the ground and placed approximately 5.5 m from its respective 1.5 meter marked PVC pole. Each PVC pole was spray-painted red and marked with 1 cm and 10 cm increments. The cameras captured images of the poles every 15-minutes for the duration of the study period. Snow depth was derived by manual inspection of the photos and recorded to the nearest cm. Daily precipitation and mean temperature data were collected for the season by a NOAA Office of Oceanic and Atmospheric Research U.S. Climate Reference Network (USCRN) station (NH Durham 2 SSW) located in the western portion of the field.

3.3 Physical land characteristics

Land and soil characteristic variables are investigated as physical drivers of field scale spatial structure of snow depth. The variables used in this study are plant functional type, slope, aspect, shadow hours, saturated hydraulic conductivity (K_{sat}), and organic matter (**Figure 1**). Mapped at a one-meter scale, all physical variables are derived from UAS snow-off observations except the two soil variables. Vegetation cover type (field/forest) was manually delineated in geographic information system

https://doi.org/10.5194/egusphere-2024-1530
Preprint. Discussion started: 21 June 2024

(GIS) software based on the image orthomosaics created during SfM processing. The forested area was further classified as coniferous or deciduous for the study region by applying the Green Leaf Index (GLI) (Louhaichi, Borman, and Johnson 2001) (**Error! Reference source not found.**) to the optical three-band (red, green, and blue) orthomosaics derived from the snow-off DJI Phantom 4 RTK survey.

$$\mathrm{GLI} = \frac{(\mathrm{Green}-\mathrm{Red})+(\mathrm{Green}-\mathrm{Blue})}{(2*\mathrm{Green})+\mathrm{Red}+\mathrm{Blue}} \quad (1)$$

The GLI algorithm delineated the dense vegetation (conifer trees) from the less dense leaf-off deciduous trees (Borman, and Johnson, 2001). The direct application of the GLI algorithm on the three-band orthomosaics was further filtered and refined as follows. The output was clustered using the k-means algorithm with number of k classes equal to two: one class for coniferous trees (high GLI) and one class for deciduous trees (low GLI). Noise within the clustered GLI map was removed by convolution with a median filter. To establish continuous delineations of coniferous regions, morphological closing was applied to the map to fill in any interior holes within the delineated regions.

The slope and aspect are derived from the UAS lidar 1 m snow-off DEM using Horn's method (Horn, 1981). The shadow hours represent the number of hours from 7 am to 5 pm that experience shadowing and was calculated using the unfiltered UAS lidar digital terrain model and the sun's incidence angle. The two soil variables, K_{sat} and organic matter, are at soil depth of 0–5 cm obtained from Probabilistic Remapping of SSURGO (POLARIS) maps at 30-m spatial resolution (Chaney et al., 2016; 2019). The soil maps were disaggregated to 1-m spatial resolution without employing interpolation methods to mitigate additional uncertainties.

3.4 Relative difference concept

The relative difference concept, first introduced by Vachaud et al. (1985), has been widely used in the soil moisture remote sensing community to quantify spatio-temporal variability (or stability) of soil moisture at field or regional scales (Cho and Choi, 2014; Cosh et al., 2004; Jacobs et al., 2004; Mohanty & Skaggs, 2001; Starks et al., 2006). In this study, we apply this concept to the UAS-lidar snow depth measurements. The relative difference in the snow depth measurements can be expressed as

$$RD_{i,t} = \frac{SND_{i,t} - spatial\ mean(SND_t)}{spatial\ mean(SND_t)} \quad (2)$$

where $SND_{i,t}$ is individual snow depth measurement at grid i and date t, and spatial mean (SND_t) is the spatial mean value of snow depth at date t. For each grid i, the mean relative difference (MRD_i) is the average relative difference from each of the N flights and can be calculated by

$$MRD_i = \frac{1}{N}\sum_{t=1}^{N} RD_{i,t} \quad (3)$$

https://doi.org/10.5194/egusphere-2024-1530
Preprint. Discussion started: 21 June 2024

4 Results

4.1 In-Situ vs UAS-measured Snow Depths

Daily temperature, daily precipitation, cumulative precipitation, and measured snow depths in the field and forest for this period are shown in **Figure** . During the 2020/2021 winter, December and early January were characterized by two ephemeral snowpacks of less than 10 cm which melted within a week. Between December 15th, 2020 and March 12th, 2021, the maximum temperature was recorded by the USCRN station on January 31st at 19° Celsius (C) and the minimum was recorded on March 11th at -19° C. The cumulative precipitation measured by the USCRN station for the winter season was 20.4 cm. A snowpack was continuously present from late January through the middle of March. The largest precipitation event captured by the USCRN station was 11 cm and occurred on January 16th. The maximum snow depth measured by the field cameras occurred on February 10th with 21 cm in the field and 19.5 cm in the forest. A second peak occurred on February 20th with 20 cm in the field and 15.5 cm in the forest. A sustained period of warm temperatures occurred in late February and early March and corresponded to a decrease in snow depth due to the warming temperatures and two rain-on-snow events. The March 7th campaign captured the transition from a snow-cover-dominated field area on March 3rd to bare ground cover-dominated.

In the field, the overall evolution of snow depth among the different measurement types shows strong agreement for the study period (**Figure**). The magnaprobe field sites typically measured deeper snow than the field camera, but otherwise, they followed a similar trend. The greatest differences in in-situ measured snow depths occurred at the beginning and end of the field season. On February 4th, the average snow depth at the magnaprobe sites was 17 cm, but the field camera only observed 4 cm of snow. On the last sample date, the magnaprobe sites had 5 cm of snow, while there was negligible snow at the field camera site. The UAS-based SfM and lidar snow depth observations were able to capture snow depth changes on the order of 5 cm or less. Neither UAS-based measurement technique consistently measured deeper or shallower snow depths than the other, regardless of snowpack depth. However, SfM snow depths across the field sites were typically much more variable than the lidar snow depths. The largest SfM standard deviations exceeded 10 cm on two dates.

https://doi.org/10.5194/egusphere-2024-1530
Preprint. Discussion started: 21 June 2024

250

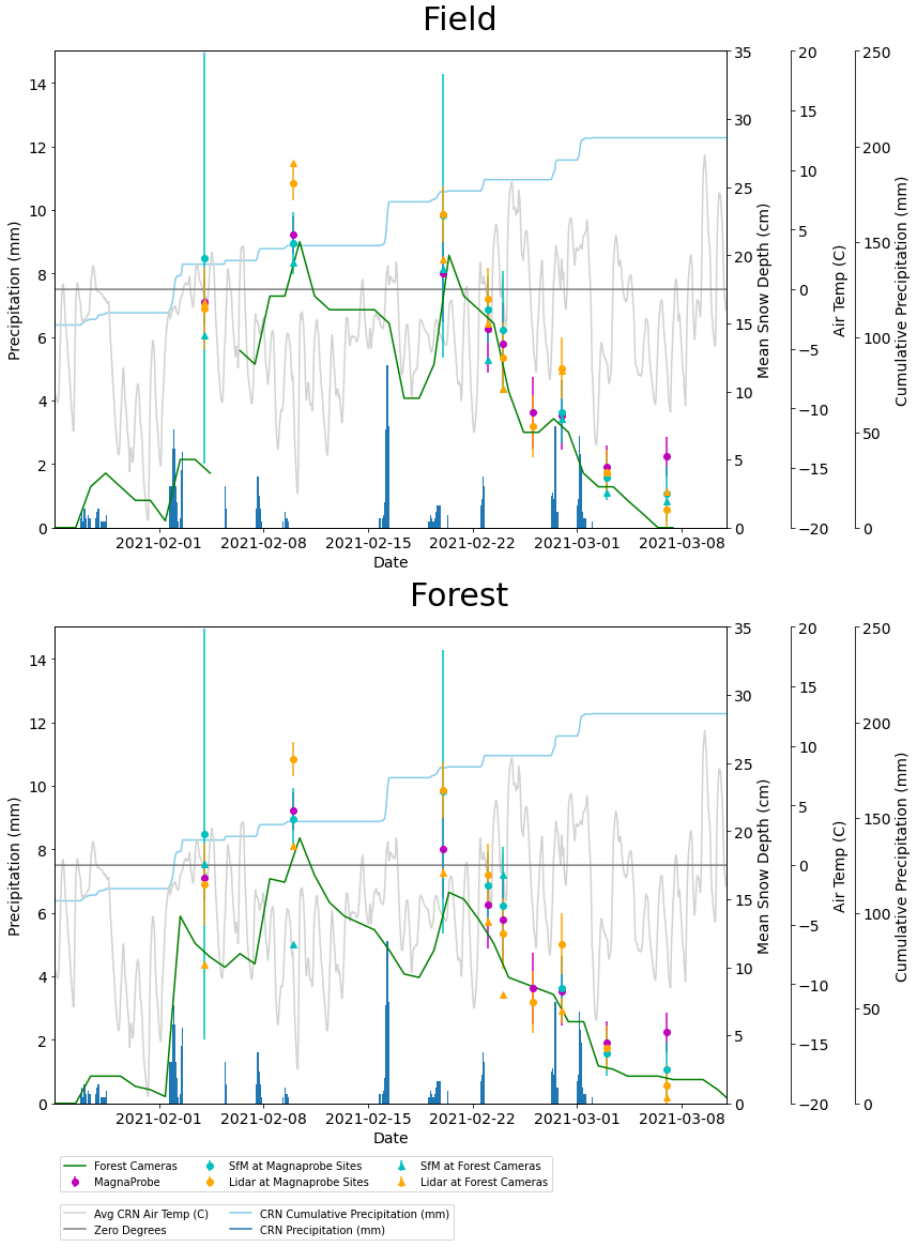

Figure 2 Timeseries of UAS-based and in-situ snow depth measurements in the field (top) and forest (bottom) for the 2021 sample season. UAS-based measurements represent average of all samples at specified sampling location (i.e., field camera, magnaprobe site).

In the forest, the trends in snow accumulation and ablation between in-situ measurement methods were similar for much of the study period, however, snow depths at the magnaprobe sites were typically much deeper than snow depths measured by the two forest cameras. During the ablation period, UAS-based measurements typically showed a decreasing snow depth that matched the progression from the in-situ measurements. However, the standard deviations for the SfM snow depths were

https://doi.org/10.5194/egusphere-2024-1530
Preprint. Discussion started: 21 June 2024

anomalously high on February 4th and February 20th. SfM snow depths had much greater variability than lidar on most days. Compared to camera and magnaprobe measurements, UAS lidar tended to underestimate snow depths whereas UAS SfM overestimated them. The SfM snow depths closely tracked the magnaprobe measurements during the ablation period.

All snow observing methods were able to distinguish that the average snow depth was slightly deeper in the forest than the field. Sensor performance was also relatively consistent in both the field and forest. The magnaprobe recorded deeper mean snow depths than the cameras in both the field (Magnaprobe = 14.2 cm, Cameras = 9.4 cm) and forest (Magnaprobe = 14.8 cm, Cameras = 9. 6 cm) (**Table A1**). In most cases, UAS-measured snow depths agreed well with in-situ measurements of snow depth regardless of the location (**Figure 3**). However, samples from the field indicated better agreement (i.e., fewer outliers) between UAS and in-situ measurements than the forest. Lidar measurements typically had less deviation from the 1:1 line than SfM, indicating that lidar performed better than SfM compared to in-situ observations, especially in the forest. Most outliers were a result of SfM overestimating snow depth compared to in-situ measurements.

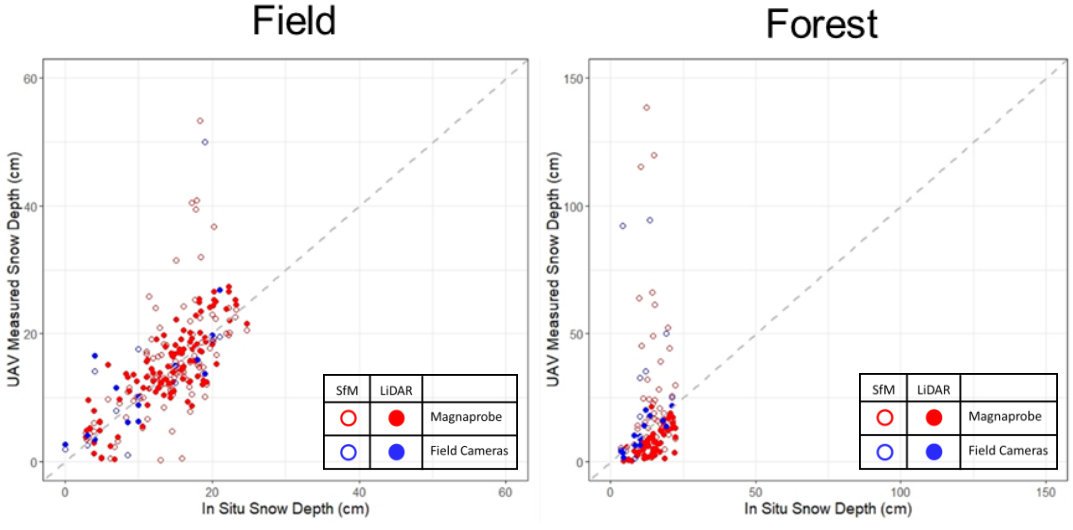

Figure 3 Comparison of UAV and in-situ based snow depth measurements for the field (left) and forest (right).

Summary statistics (**Table A1**) indicate that the UAS lidar outperformed the UAS SfM in both the field and forest. SfM snow depths had higher mean absolute error (MAE) than the lidar as compared to the magnaprobe (SfM = 5.0 cm, Lidar = 3.0 cm) and the field camera (SfM = 14.3 cm, Lidar = 3.0 cm) in the field. In the forest, the MAE values increased modestly for the lidar, but sharply for the SfM snow depths when compared to both the magnaprobe observations (SfM = 32.0 cm, Lidar = 7.3 cm) and the two camera observations (SfM = 44.7 cm, Lidar = 2.7 cm). In addition, lidar measurements had a greater r^2 value than SfM at all the magnaprobe sites in the field (SfM = 0.33, Lidar = 0.65) and the forest (SfM = 0.01, Lidar = 0.41) and all camera sites in the field (SfM = 0.06, Lidar = 0.71) and the forest (SfM = 0.01, Lidar = 0.80).

https://doi.org/10.5194/egusphere-2024-1530
Preprint. Discussion started: 21 June 2024

4.2 Comparison between LiDAR and SfM Snow Depth

A direct comparison between the snow depths measured by lidar and SfM was conducted over the entire study area, encompassing four segmented areas. The overlapping 1 m x 1 m snow depth pixel values for the two UAS techniques were compared (Error! Reference source not found.). In both the field and forest, SfM snow depth frequently recorded much deeper s now than the lidar. Compared to the northwestern (NW) and eastern (E) portions of the field, the western (W) field area had the most similar snow depth values for SfM and lidar. In that field, both lidar and SfM techniques captured relatively deeper snow depths ranging from 50 to 100 cm. However, there was no clear agreement between SfM and lidar in the forest, largely due to extensive regions in which SfM snow depths were anomalously high.

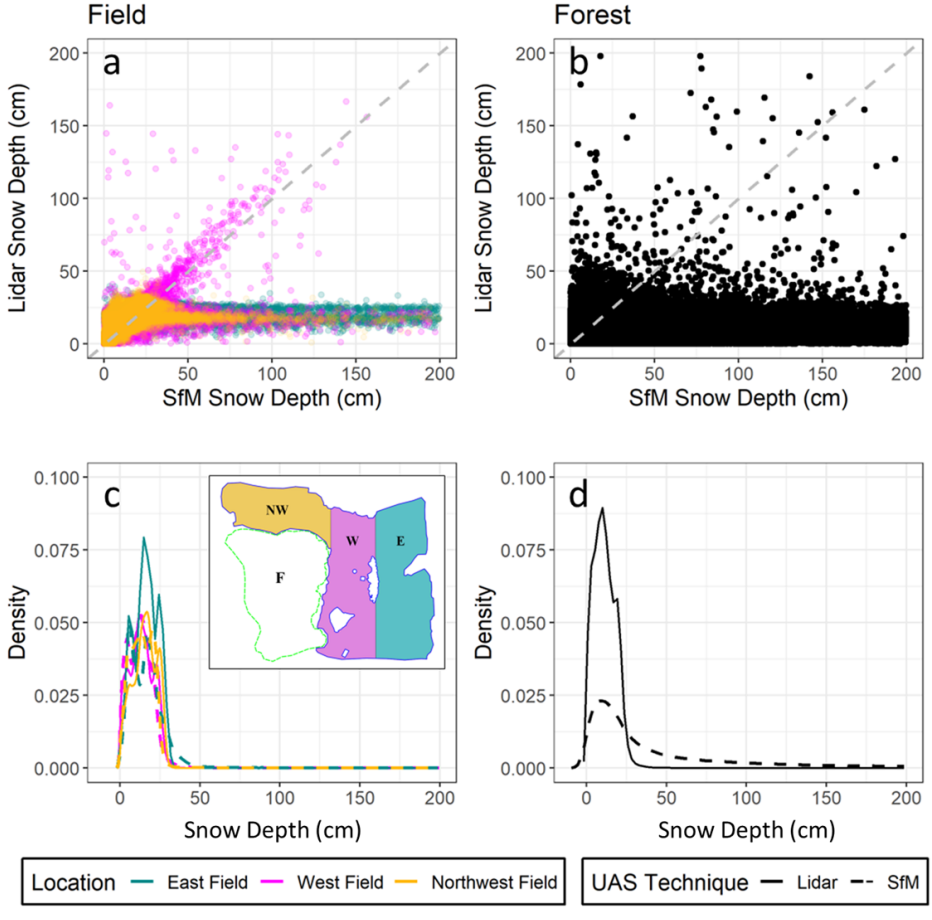

Figure 4 Comparison of SfM and lidar measurements for all sample dates by area. Top scatter plots compare snow depth for (a) the three field areas and (b) the forest area. Bottom probability density plots show the distribution of snow depth values for (c) the field and (d) the forest area by measurement type.

https://doi.org/10.5194/egusphere-2024-1530
Preprint. Discussion started: 21 June 2024

A timeseries of snow depth maps for lidar and SfM over the entire sample area are shown in Error! Reference source not found.. The difference between the snow depths maps for each technique was calculated for each sample date to identify
285 locations where the techniques had the greatest difference in measured snow depths. There was an overall trend of decreasing snow depth over time in both the field and forest areas. The spatial difference between SfM and lidar was fairly consistent in the field on each day (approximately 0 cm) except for February 20th and 24th where the southeastern field showed a negative difference compared to other sample dates. It was clear that areas of missing data (such as that on February 4th) had a significant impact on results. In the forest, missing or patchy SfM data were found on many days (e.g., February 4th and 28th).

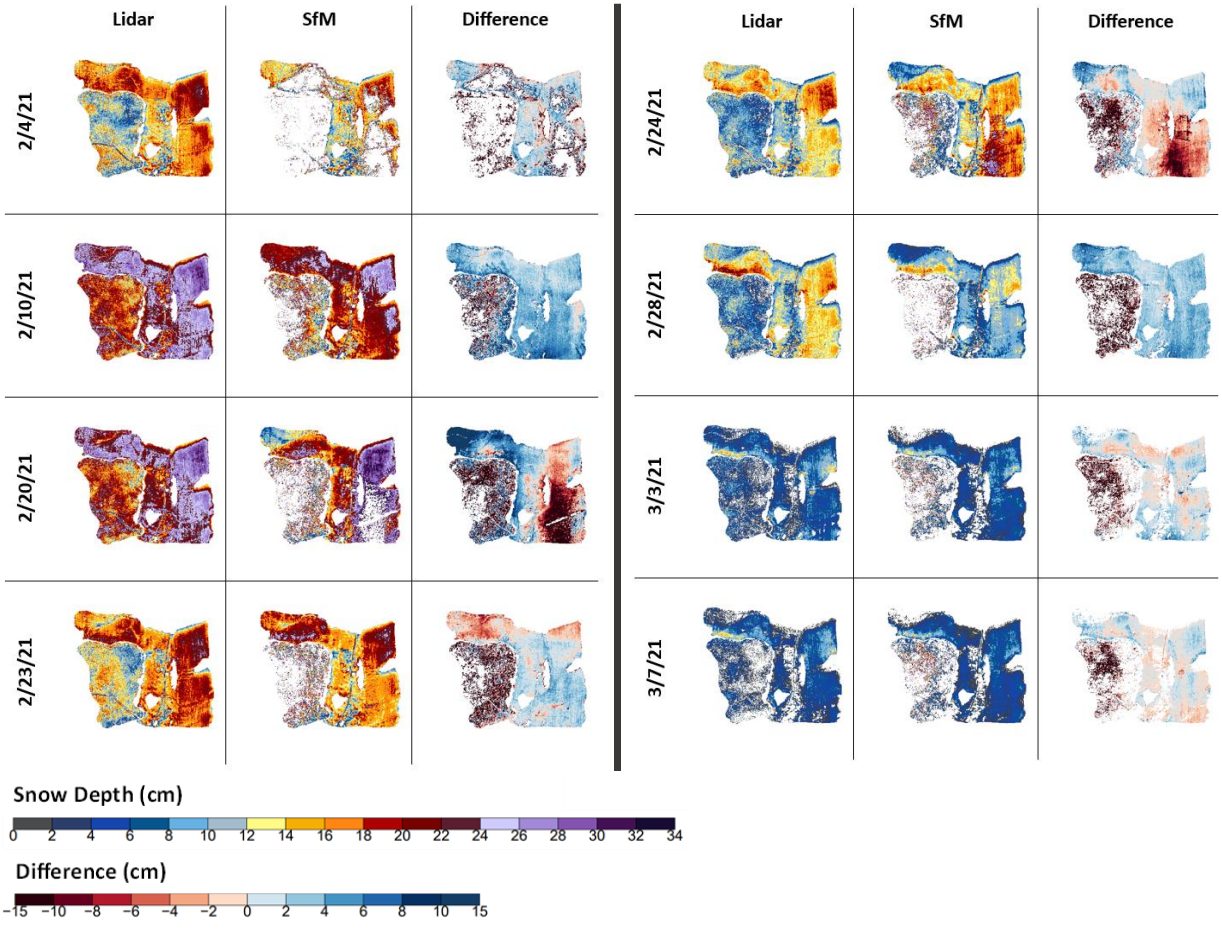

Figure 5 Time series of snow depths (SD) for Lidar and SfM in the field and forest. Difference is calculated as Lidar SD minus SfM SD. All values shown in cm.

https://doi.org/10.5194/egusphere-2024-1530
Preprint. Discussion started: 21 June 2024

290 **4.3 Spatial Structure of Snowpack and its Temporal Changes**

To explore the spatial structure of snow depth over time, daily relative difference of snow depth maps were generated from the UAS lidar-based snow depth maps (**Figure 6**). The spatial patterns of relative differences were fairly consistent throughout the period. Generally, there was relatively deeper snow depth in the northern part of the field (about 50% larger than the spatial mean), and shallower snow depth was found in forested areas as well as the central part of the field. Also, there were shallower
295 snow depth measurements along the northeastern boundaries of the field. These patterns were very clear during the accumulation period before the peak snow depth around February 22nd. During the ablation period, the patterns were still consistent even though there were some gaps with no snow present because of patchy snow. This indicates that there are minimal changes in spatial structure of snow depth over the season in this environment.

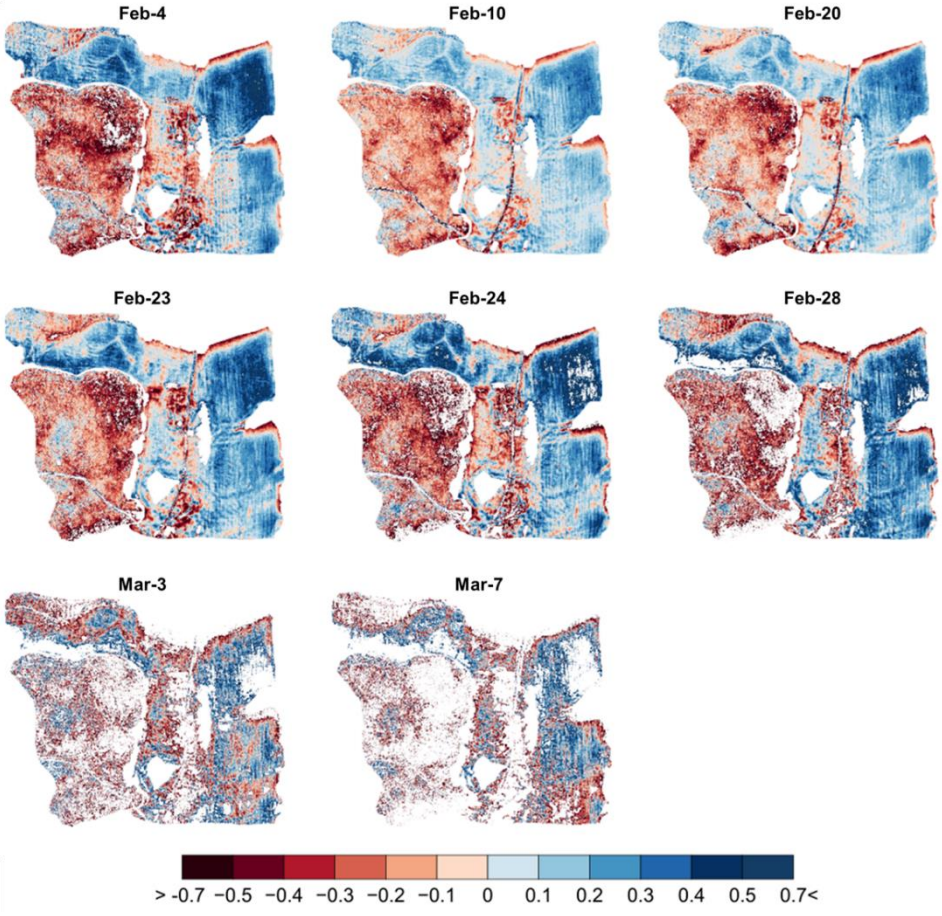

Figure 6 Relative difference (RD) maps generated from the UAS lidar-based SD maps from February 4th to March 7th.

The MRD map in **Figure 7** show the average spatial structure of snow depth formed in the study domain over the time period.
300 The field had relatively deeper snow depths by up to 70% relative to the spatial mean. Within the field, the snow depth in northern areas was generally deeper than that in the southern areas, except for near the northern edges where it was generally shallower. In forested areas, the snow depth was shallower by up to -70% relative to the spatial mean. Distinct differences in

https://doi.org/10.5194/egusphere-2024-1530
Preprint. Discussion started: 21 June 2024

the transition zones between field and forest show edge effects. A shallower snowpack is evident immediately south of the forest at the northern extent of the field. There is a transition zone with deepening snow with increasing distance from the forest edge. In the western field, markedly deeper snow is found north of the forest.

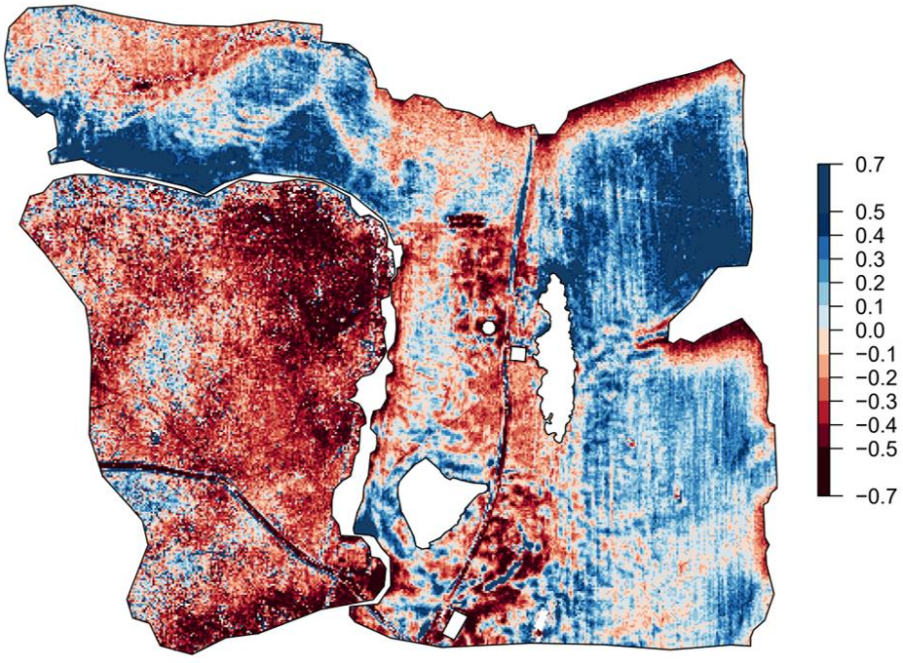

Figure 7 The snow depth Mean Relative difference (MRD) map generated by averaging the eight RD maps from the UAS lidar-based snow depth maps from February 4th to March 7th.

4.4 Physical Variables Characterizing Spatial Structures of Snow Depth

To evaluate the effect of physical land characteristics on the spatial structure of snow depth, the MRD values were analyzed with respect to five land and soil characteristic values (e.g., vegetation type, slope, shadow hours, K_{sat}, and soil organic matter) over the study domain (**Figure 8**). Boxplots of MRD by physical feature are shown for the combined forest and field areas (**Figure 8a**) and field only (**Figure 8b**). In the combined areas (i.e., forest + field), the snow spatial structure is primarily controlled by vegetation type. Coniferous forests have low MRDs (mean: -0.36) which means snow in those areas is shallower relative to the spatial mean of snow depth by around 36%. For the deciduous forest, the mean MRD is -0.2 with a wide quantile range from –0.23 to 0.19. MRD values in the field are higher compared to the two forest types which ranged from –0.11 to 0.22 (mean: 0.08). For both cases, the combined areas and field only, slope contributes to snowpack spatial patterns, even though the study area has gentle slope (less than 20%). High MRDs are found in flat areas (0 – 5% slope) and gradually decrease with increasing slope. The shadow hours show a clear but contradictory contribution to snow depth patterns in the field area and the combined area. In field, low MRDs are found in areas where shadow hours are short (e.g., less than 2 hours), and the MRDs gradually increase with increasing shadow hours. For the combined area, the highest shadow had the lowest

https://doi.org/10.5194/egusphere-2024-1530
Preprint. Discussion started: 21 June 2024

320 snow depth, but this is likely the result of a mixed effect due to the dense shading in the coniferous forest. K_{sat} shows little evidence of contributing to the spatial structure of snow depth in the field. In the combined areas, the MRDs seem to decrease with increasing the K_{sat} values, except for the highest K_{sat} group, there are no significant patterns of MRDs when field areas are analyzed only. Compared to K_{sat}, soil organic matter (SOM) has a clearer relationship showing that snow depth decreases with increasing SOM in both the combined areas and field analysis.

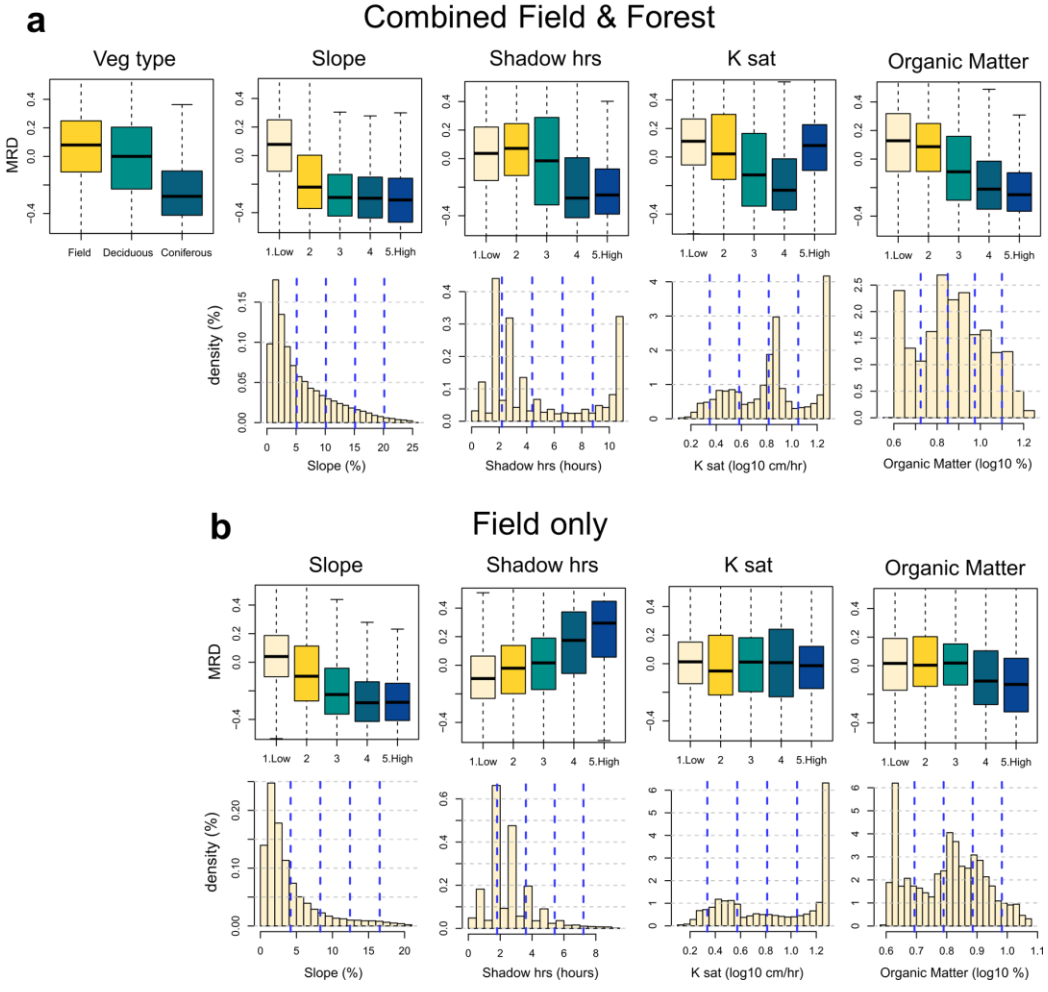

Figure 8 Boxplots of the snow depth Mean Relative difference (MRD) by each physical feature (vegetation type, slope, shadow hours, K_{sat}, and soil organic matter) for the combined areas (forest and field) and field only.

325

https://doi.org/10.5194/egusphere-2024-1530
Preprint. Discussion started: 21 June 2024

5 Discussion

5.1 Comparison with previous findings: UAS SfM and LiDAR snow depths

The value of lidar datasets for capturing the horizontal and vertical structure of forests and snow cover depth is well established. However, the technology remains expensive and data processing is complex. UAV SfM provides a low-cost alternative to lidar for creating point clouds using photogrammetry. However, its accuracy for measuring forest snow depths is still being explored (Donager et al. 2021). The lower cost of SfM techniques compared to lidar make them a valuable tool for conducting surveys of snowpack change over time. Post-processing of RGB imagery is often less complex than lidar data processing, and a variety of SfM software is now available, including some open-source options. While it is apparent that the accuracy of SfM-derived snow depth estimates cannot match that of lidar, the results of this study indicate that they can provide sufficient accuracy for investigation of flat, unforested land cover types. However, specific conditions which influence the relative performance of SfM for measuring snow depths in these areas, such as that observed in the western field, were still unclear. One potential reason for this could be overcast skies and features that present challenges for SfM processing, whereas lidar is less impacted by these challenges.

Compared to in-situ measurements, SfM experienced modestly higher error in the field and notably higher errors in the forest than lidar. In SfM processing, an insufficient number of point clouds in the field may degrade the accuracy of SfM SD data (Harder et al., 2016). The direct comparison of SfM and lidar measurements revealed that, despite SfM typically measuring deeper snow depths than lidar, both SfM and lidar had better agreement in the field than the forest. However, the techniques did not have consistent agreement over the entire field, with the best agreement occurring in the western portion of the field. These findings are similar to previous studies which compared UAS SfM and snow probe measurements where the RMSE for snow depths is typically less than 31 cm in sparsely vegetated and alpine land cover types and increases to as much as 37 cm in areas with bushes, high grass, or forests (De Michele et al., 2016, Bühler et al., 2016, Avanzi et al., 2018, Belmonte et al., 2021). Studies using UAS SfM alongside rulers and snow stakes measured a smaller RMSE (less than 14 cm) in both forested and prairie land cover types (Fernandes et al., 2018; Harder et al., 2016). Findings were also similar for studies comparing UAS lidar to rulers or snow stakes which measured a RMSE less than 17 cm, with even lower RMSE in shallow snow and in sunny areas (Harder et al., 2020; Feng et al., 2023; Koutantou et al., 2022). Lidar RMSE also tends to increase in vegetated areas regardless of the vegetation class or type (Harder et al. 2020). Much like the erroneous SfM snow depth measurements observed by Harder et al. (2016) several meters above the snow surface, we observed SfM measured snow depths were greater than 150 cm in some forest locations. Conversely, lidar measured snow depths never exceeded 25 cm, indicating a more consistent performance in forested areas.

Regardless of the sampling technique used, the unique capability of UAS for measuring snowpack properties at the field-scale at a high temporal-resolution makes them useful for observing snowpack evolution over time. Collection of in-situ snow depth timeseries data is often time and cost prohibitive and may be especially challenging in complex or avalanche-

https://doi.org/10.5194/egusphere-2024-1530
Preprint. Discussion started: 21 June 2024

prone terrain. It is clear from the results of this study and previous ones that both UAS SfM and lidar techniques provide a viable method for monitoring snow depth change across many land cover types. Monitoring snow depth change over time at the field scale allowed for identification of accumulation and ablation patterns across the entire study area and between different land cover types (i.e., forest and field). Comparing maps of snow depth change to maps of the physical variables present at the site revealed the specific variables which may influence snowpack change over the winter season.

5.2 Physical variables at field scale

With a limited wind redistribution, time stability shows that the relative differences of the snowpack over the study region were generally stable throughout the accumulation and melting periods. In addition to the previous findings that snowpack patterns are relatively consistent from year to year (Pflug and Lundquist, 2020; Revuelto et al., 2014), this study showed that fixed physical variables including vegetation, topography, and soil characteristics sufficiently control the spatial variations of snowpack throughout a winter period. The findings regarding the influence of vegetation and topographical factors on the snowpack's spatial variability align with previous studies conducted (Currier and Lundquist, 2018; Deems et al., 2006; Trujillo et al., 2007). As compared to vegetation and terrain characteristics, few studies have examined the influence of soil characteristics on the snowpack. Our results found that snowpack depth decreases with increasing soil organic matter. This finding aligns with our previous study, which utilized maximum entropy modeling to analyze spatial variations of shallow snowpack over the same domain but during different periods (Cho et al., 2021). Even though a clear relationship between saturated hydraulic conductivity and snowpack was not found in this study (**Figure 8b**), it is acknowledged that soil thermal properties, such as the thermal conductivity of the soil beneath the snowpack, generally influence the rate of heat transfer between the snow and soil layers (Kane et al., 2001; Zhang, 2005). Also, the moisture content of the soil can affect the distribution of soil frost (Bay et al., 1952) and snowpack because the energy transfer at the snow-soil interface is controlled by wetness of the soil (Bay et al., 1952; Fu et al., 2018). Even though spatial distribution of soil moisture contents is typically considered to be constant (frozen) during winter, intermediate rainfall events and freeze-thaw cycles can dramatically change the spatial patterns of soil moisture and freeze-thaw states. This can be critical because the thermal conductivity in frozen state is more sensitive to soil type than non-frozen condition, because the thermal conductivity of ice is four times larger than that of liquid phase (Penner, 1970). However, fewer studies have investigated how soil moisture patterns may control the spatial structure of snowpack. This is likely because of the difficulty of measuring spatial distributions of soil moisture and freeze-thaw states beneath the snowpack. Even though this study did not focus on it, future investigations could measure spatial patterns of soil moisture and freeze-thaw states beneath the snowpack to quantify their interactions with the snowpack. A better understanding of the soil characteristics and their impact on the snowpack in various environments would help snow community accurately predict and model snow distribution and snowmelt processes.

The concept of "time stability" (or "temporal stability") implemented in this study has not been used in snow hydrology, though there are numerous studies using similar concepts to characterize temporal changes in the spatial structure of snowpack across topographically uniform landscapes, encompassing both open field and forested environments. The

https://doi.org/10.5194/egusphere-2024-1530
Preprint. Discussion started: 21 June 2024

numerous investigations in the soil moisture community that have examined temporal variability were valuable for developing robust validation sites and sampling strategies for satellite-based soil moisture assessments (Grayson and Western, 1998; Cosh et al., 2008; Brocca et al., 2009; Mohanty & Skagge, 2001; Jacobs et al., 2004). Similar to its utility in soil moisture studies, the integration of the time stability concept into snowpack analysis at the field scale could facilitate the identification of representative sampling locations and inform the design of sampling protocols for optimal spatial extrapolation. Extending this approach to diverse snow environments will contribute to quantifying spatio-temporal variability in snowpack, thereby enhancing the establishment of core validation sites for potential snow missions such as the Canadian Terrestrial Snow Mass Mission (TSMM; Derksen et al., 2019).

5.3 Limitations and future perspectives

Given that our investigation was conducted in a relatively uniform landscape characterized by a shallow snowpack, it is imperative to extend the analysis to encompass diverse plant functional types, climatic zones, and/or snow classes (Johnston et al., 2024; Sturm and Liston, 2021) to ascertain the generalizability of the findings. This is essential as snow depth distributions are influenced by terrain attributes and snow regimes (Clark et al., 2011; Currier and Lundquist, 2018). In contrast to the present study area, where spatial heterogeneity in snowpack is predominantly influenced by static terrain characteristics and vegetation cover, alpine and prairie regions experience variability due to wind-driven processes (Elder et al., 1991). Further investigation incorporating additional analyses of energy fluxes and meteorological parameters, including solar radiation, soil temperature and wind speed/direction, would enhance the comprehensiveness of the findings concerning the primary determinants of snowpack spatial variability across both static and dynamic variables.

Even though we analyzed spatial-temporal variability of snowpack using a well-validated UAS-based snow depth, this may not guarantee similar results with snow water equivalent (SWE) that would be necessary for hydrologic applications. Snow density, needed to calculate SWE from snow depth, is affected by snow metamorphosis differently than snow depth . Snow density may change during snowmelt as water percolates into the snowpack and refreezes. Also, vegetation and soil characteristics strongly control turbulent and ground heat fluxes and impact snow properties including snow density (Pomeroy and Brun, 2001). Studies have used a snow modeling approach using physics-based sophisticated models such as SnowModel (Liston and Elder, 2006) and Crocus (Vionnet et al., 2012) to understand those SWE patterns with physical processes how spatial variations of snowpack are formed. However, observational approaches focusing on spatial structures of SWE are quite limited because only now are sensing techniques emerging that directly observe the spatial distribution of snow density with a UAS system (McGrath et al., 2022). A potential future direction is to develop reliable, high-resolution SWE maps by integrating emerging techniques such as lidar and gamma-ray spectrometry (Harder et al., 2023), enabling the quantification of spatial structures of SWE across diverse snow environments. Another direction could involve employing an integrative approach using physical models to maximize in-situ and UAS snow observations through data assimilation and/or novel interpolation methods, utilizing machine (or deep) learning approaches.

https://doi.org/10.5194/egusphere-2024-1530
Preprint. Discussion started: 21 June 2024

6 Conclusion

In this study, UAS lidar and SfM snow depth measurements were assessed using the ground-based magnaprobe and field cameras then used to confirm that spatial patterns of snowpack depth are temporal stable. Differences between in-situ measurement techniques had only a modest impact on validation of lidar and SfM-based snow depth. Lidar demonstrated superior performance compared to SfM when evaluated against in-situ observations, exhibiting lower errors. Both UAS techniques exhibited lower errors in field settings than in forested environments. Though, as expected, differences between lidar and SfM snow depths were more pronounced in forested regions, with SfM often registering anomalously deep snow depth values. The spatial structures of snow depth captured by lidar remained consistent throughout the study period and were primarily influenced by factors such as vegetation type, slope, shadow hour, and soil organic matter. When examining combined landscapes including forests and fields, we observed that the spatial structure of snow depth was predominantly shaped by the type of vegetation present. Within the field, the spatial distribution of snow depth tracked with relatively modest local slope variations and shadowing effects at the forest-field edge. As ephemeral snow conditions expand in a warmer climate, these results are valuable for effectively comparing UAS and in-situ sampling techniques for ephemeral, shallow seasonal snowpacks. It is also expected that this study contributes to the enhancement of land surface and snow models by offering insights into parameterizing sub-grid scale snow depths, downscaling coarse-scale remotely sensed snow observations, and comprehending snowpack evolution at the field scale, particularly in ephemeral snow environments.

Data availability. The UAS lidar and SfM photogrammetry snow depth maps, along with topographic variables developed in this study, will be available for download from the Hydroshare repository once this manuscript is accepted and published (currently being set up with an ODC Attribution license for unrestricted access). Daily precipitation and mean temperature data are available from the NOAA U.S. Climate Reference Network at https://www.ncei.noaa.gov/access/crn/sensors.htm?stationId=1040.

Author contributions. EC, MV, JMJ, and AH conceptualized the research, conducted the formal analysis, and wrote the initial draft. FS, MP, and CW assisted with fieldwork and investigation, providing technical and scientific inputs. JMJ supervised the project. All authors reviewed and edited the paper.

Competing interests. On behalf of all authors, the corresponding author states that there is no conflict of interest

Acknowledgments. This study is based upon work supported by the U.S. Department of Defense Engineer Research and Development Center's Broad Agency Announcement (BAA) #W912HZ20BAA01 and the U.S. Army ERDC's Cold Region Research and Engineering Laboratory (CRREL) under contract number W913E5-21-C-0006. Any opinions, findings, and conclusions or recommendations in this material are those of the authors and do not necessarily reflect the views of the Broad

https://doi.org/10.5194/egusphere-2024-1530
Preprint. Discussion started: 21 June 2024

Agency Announcement Program and the ERDC-CRREL. DISTRIBUTION A: Approved for Public Release. Distribution is Unlimited. The authors are grateful to Elizabeth Burakowski, Mahsa Moradi Khaneghahi, and Holly Proulx for helping data collection and providing valuable comments.

References

Anderton, S.P., White, S.M., Alvera, B.: Micro-scale spatial variability and the timing of snow melt runoff in a high mountain catchment. J. Hydrol. 268 (1-4), 158–176, https://doi.org/10.1016/S0022-1694(02)00179-8, 2002.

Avanzi, F., Bianchi, A., Cina, A., De Michele, C., Maschio, P., Pagliari, D., et al.: Centimetric accuracy in snow depth using unmanned aerial system photogrammetry and a multistation. Remote Sensing, 10(5), 76, https://doi.org/10.3390/rs10050765, 2018.

Barnett, T.P., Adam, J.C., Lettenmaier, D.P.: Potential impacts of a warming climate on water availability in snow-dominated regions. Nature, 438 (7066), 303–309, 2005.

Bay, C.E., Wunnecke, G.W. and Hays, O.E.: Frost penetration into soils as influenced by depth of snow, vegetative cover, and air temperatures. Eos, Transactions American Geophysical Union, 33(4), 541-546, 1952.

Belmonte, A., Sankey, T., Biederman, J., Bradford, J., Goetz, S., & Kolb, T.: UAV-based estimate of snow cover dynamics: Optimizing semi-arid forest structure for snow persistence. Remote Sensing, 13(5), 1036, 2021.

Boelman, N. T., Liston, G. E., Gurarie, E., Meddens, A. J., Mahoney, P. J., Kirchner, P. B., et al.: Integrating snow science and wildlife ecology in Arctic-boreal North America. Environmental Research Letters, 14(1), 010401, 2019.

Brocca, L., Melone, F., Moramarco, T., & Morbidelli, R.: Soil moisture temporal stability over experimental areas in Central Italy. Geoderma, 148(3-4), 364-374, 2009.

Burakowski, E.A., Ollinger, S.V., Lepine, L., Schaaf, C.B., Wang, Z., Dibb, J.E., et al.: Spatial scaling of reflectance and surface albedo over a mixed-use, temperate forest landscape during snow-covered periods. Remote Sens. Environ. 158, 465–477. https://doi.org/10.1016/j.rse.2014.11.023, 2015.

Burakowski, E., Hamilton, L.: Are New Hampshire's Winters Warming? Yes, but fewer than half state residents recognize the trend, Regional Issue Brief #61. Carsey School of Public Policy, University of New Hampshire. https://doi.org/10.34051/p/ 2020.377, 2020.

Bühler, Y., Adams, M. S., Bösch, R., & Stoffel, A.: Mapping snow depth in alpine terrain with unmanned aerial systems (UASs): potential and limitations. The Cryosphere, 10(3), 1075-1088, 2016.

Carroll, R.W.H., Deems, J.S., Niswonger, R., Schumer, R., Williams, K.H.: The importance of interflow to groundwater recharge in a snowmelt-dominated headwater basin. Geophys. Res. Lett. 46 (11), 5899–5908, 2019.

Chaney, N.W., Minasny, B., Herman, J.D., Nauman, T.W., Brungard, C.W., Morgan, C.L. S.: POLARIS soil properties: 30-m probabilistic maps of soil properties over the contiguous United States. Water Resour. Res. 55 (4), 2916–2938, 2019.

Chaney, N.W., Wood, E.F., McBratney, A.B., Hempel, J.W., Nauman, T.W., Brungard, C. W.: POLARIS: A 30-meter probabilistic soil series map of the contiguous United States. Geoderma 274, 54–67, 2016.

https://doi.org/10.5194/egusphere-2024-1530
Preprint. Discussion started: 21 June 2024

Cho, E., Hunsaker, A. G., Jacobs, J. M., Palace, M., Sullivan, F. B., & Burakowski, E. A.: Maximum entropy modeling to identify physical drivers of shallow snowpack heterogeneity using unpiloted aerial system (UAS) lidar. Journal of Hydrology, 602, 126722, https://doi.org/10.1016/j.jhydrol.2021.126722, 2021.

Cho, E., & Choi, M.: Regional scale spatio-temporal variability of soil moisture and its relationship with meteorological factors over the Korean peninsula. Journal of Hydrology, 516, 317-329, 2014.

Cho, E., Kwon, Y., Kumar, S. V., and Vuyovich, C. M.: Assimilation of airborne gamma observations provides utility for snow estimation in forested environments, Hydrol. Earth Syst. Sci., 27, 4039–4056, https://doi.org/10.5194/hess-27-4039-2023, 2023.

Clark, M.P., Hendrikx, J., Slater, A.G., Kavetski, D., Anderson, B., Cullen, N.J.: Representing spatial variability of snow water equivalent in hydrologic and land-surface models: A review. Water Resour. Res. 47 (7) https://doi.org/10.1029/2011WR010745, 2011.

Cosh, M. H., Jackson, T. J., Bindlish, R., & Prueger, J. H.: Watershed scale temporal and spatial stability of soil moisture and its role in validating satellite estimates. Remote Sensing of Environment. doi: 10.1016/j.rse.2004.02.016, 2004.

Currier, W. R., & Lundquist, J. D.: Snow depth variability at the forest edge in multiple climates in the western United States. Water Resources Research, 54(11), 8756-8773, 2018.

Deems, J. S., Fassnacht, S. R., & Elder, K. J.: Fractal distribution of snow depth from lidar data. Journal of Hydrometeorology, 7(2), 285-297, 2006.

De Michele, C., Avanzi, F., Passoni, D., Barzaghi, R., Pinto, L., Dosso, P.: Using a fixed-wing UAS to map snow depth distribution: an evaluation at peak accumulation. The Cryosphere, 10(2), 511-522, 2016.

Derksen, C., Walker, A., & Goodison, B. (2005). Evaluation of passive microwave snow water equivalent retrievals across the boreal forest/tundra transition of western Canada. Remote sensing of environment, 96(3-4), 315-327.

Derksen, C., Lemmetyinen, J., King, J., Belair, S., Garnaud, C., Lapointe, M.: A dual-frequency ku-band radar mission concept for seasonal snow. In IGARSS 2019-2019 IEEE International Geoscience and Remote Sensing Symposium (pp. 5742-5744). IEEE, 2019.

Donager, J., Sankey, T. T., Meador, A. J. S., Sankey, J. B., & Springer, A.: Integrating airborne and mobile lidar data with UAV photogrammetry for rapid assessment of changing forest snow depth and cover. Science of Remote Sensing, 4, 100029, 2021.

Elder, K., Dozier, J., & Michaelsen, J.: Snow accumulation and distribution in an alpine watershed. Water Resources Research, 27(7), 1541-1552, 1991.

Feng, T., Hao, X., Wang, J., Luo, S., Huang, G., Li, H., & Zhao, Q.: Applicability of alpine snow depth estimation based on multitemporal UAV-LiDAR data: A case study in the Maxian Mountains, Northwest China. Journal of Hydrology, 617, 129006, 2023.

Fernandes, R., Prevost, C., Canisius, F., Leblanc, S. G., Maloley, M., Oakes, S.: Monitoring snow depth change across a range of landscapes with ephemeral snowpacks using structure from motion applied to lightweight unmanned aerial vehicle videos. The Cryosphere, 12(11), 3535-3550, 2018.

Fu, Q., Hou, R., Li, T., Wang, M., & Yan, J.: The functions of soil water and heat transfer to the environment and associated response mechanisms under different snow cover conditions. Geoderma, 325, 9-17, 2018.

https://doi.org/10.5194/egusphere-2024-1530
Preprint. Discussion started: 21 June 2024

Gaffey, Clare, and Anshuman Bhardwaj.: Applications of Unmanned Aerial Vehicles in Cryosphere: Latest Advances and Prospects., Remote Sensing 12 (948). https://doi.org/doi:10.3390/rs12060948, 2020.

Grayson, R. B., & Western, A. W.: Towards areal estimation of soil water content from point measurements: time and space stability of mean response. Journal of Hydrology, 207(1-2), 68-82, 1998.

Grayson, R.B., Blöschl, G., Western, A.W., McMahon, T.A.: Advances in the use of observed spatial patterns of catchment hydrological response. Adv. Water Resour. 25 (8-12), 1313–1334, 2002.

Grogan, D. S., Burakowski, E. A., & Contosta, A. R.: Snowmelt control on spring hydrology declines as the vernal window lengthens. Environmental Research Letters, 15(11), 114040, 2020.

Harder, P., Helgason, W., and Pomeroy, J.: Measuring prairie snow water equivalent with combined UAV-borne gamma spectrometry and lidar, EGUsphere, https://doi.org/10.5194/egusphere-2023-2586, 2023.

Harder, P., Pomeroy, J. W., & Helgason, W. D.: Improving sub-canopy snow depth mapping with unmanned aerial vehicles: lidar versus structure-from-motion techniques. The Cryosphere, 14(6), 1919-1935, 2020.

Harder, P., Schirmer, M., Pomeroy, J., & Helgason, W.: Accuracy of snow depth estimation in mountain and prairie environments by an unmanned aerial vehicle. The Cryosphere, 10(6), 2559-2571, 2016.

Harpold, A.A., Molotch, N.P., Musselman, K.N., Bales, R.C., Kirchner, P.B., Litvak, M. et al.: Soil moisture response to snowmelt timing in mixed-conifer subalpine forests. Hydrol. Process. 29 (12), 2782–2798, 2015.

Harpold, A. A., Kaplan, M. L., Klos, P. Z., Link, T., McNamara, J. P., Rajagopal, S., et al.: Rain or snow: hydrologic processes, observations, prediction, and research needs. Hydrology and Earth System Sciences, 21(1), 1-22, 2017.

Harrison, H. N., Hammond, J. C., Kampf, S., & Kiewiet, L.: On the hydrological difference between catchments above and below the intermittent-persistent snow transition. Hydrological Processes, 35(11), e14411, 2021.

Jacobs, J. M., Hunsaker, A. G., Sullivan, F. B., Palace, M., Burakowski, E. A., Herrick, C., et al.: Shallow snow depth mapping with unmanned aerial systems lidar observations: A case study in Durham, New Hampshire, United States. The Cryosphere, 15, 1-17, https://doi.org/10.5194/tc-2020-37, 2021.

Jacobs, J. M., Mohanty, B. P., Hsu, E. C., & Miller, D.: SMEX02: Field scale variability, time stability and similarity of soil moisture. Remote sensing of Environment, 92(4), 436-446, 2004.

Johnston, J., Jacobs, J.M. and Cho, E.: Global Snow Seasonality Regimes from Satellite Records of Snow Cover. Journal of Hydrometeorology, 25(1), 65-88, 2024.

Kane, D. L., Hinkel, K. M., Goering, D. J., Hinzman, L. D., & Outcalt, S. I.: Non-conductive heat transfer associated with frozen soils. Global and Planetary Change, 29(3-4), 275-292, 2001.

Koutantou, K., Mazzotti, G., Brunner, P., Webster, C., & Jonas, T.: Exploring snow distribution dynamics in steep forested slopes with UAV-borne LiDAR. Cold Regions Science and Technology, 200, 103587, 2022.

Lawrence, D.M., Slater, A.G.: The contribution of snow condition trends to future ground climate. Clim. Dyn. 34 (7-8), 969–981, 2010.

Lievens, H., Brangers, I., Marshall, H. P., Jonas, T., Olefs, M., & De Lannoy, G.: Sentinel-1 snow depth retrieval at sub-kilometer resolution over the European Alps. The Cryosphere, 16(1), 159-177, 2022.

https://doi.org/10.5194/egusphere-2024-1530
Preprint. Discussion started: 21 June 2024

Liston, G. E., & Elder, K.: A distributed snow-evolution modeling system (SnowModel). Journal of Hydrometeorology, 7(6), 1259-1276, 2006.

Maurer, G.E., Bowling, D.R., Seasonal snowpack characteristics influence soil temperature and water content at multiple scales in interior western US mountain ecosystems. Water Resour. Res. 50 (6), 5216–5234, 2014.

McGrath, D., Bonnell, R., Zeller, L., Olsen-Mikitowicz, A., Bump, E., Webb, R., et al.: A time series of snow density and snow water equivalent observations derived from the integration of GPR and UAV SFM Observations. Frontiers in Remote Sensing, 3, 886747, 2022.

Meyer, J., Deems, J. S., Bormann, K. J., Shean, D. E., & Skiles, S. M.: Mapping snow depth and volume at the alpine watershed scale from aerial imagery using Structure from Motion. Frontiers in Earth Science, 10, 989792, 2022.

Monson, R. K., Lipson, D. L., Burns, S. P., Turnipseed, A. A., Delany, A. C., Williams, M. W., et al.: Winter forest soil respiration controlled by climate and microbial community composition. Nature, 439(7077), 711-714, 2006.

Mott, R., Schirmer, M., Lehning, M.: Scaling properties of wind and snow depth distribution in an Alpine catchment. J. Geophys. Res.: Atmosph. 116 (D6), 2011.

Mohanty, B. P., & Skaggs, T. H.: Spatio-temporal evolution and time-stable characteristics of soil moisture within remote sensing footprints with varying soil, slope, and vegetation. Advances in Water Resources, 24, 1051 – 1067, 2001.

Painter, T. H., Berisford, D. F., Boardman, J. W., Bormann, K. J., Deems, J. S., Gehrke, F., et al.: The Airborne Snow Observatory: Fusion of scanning lidar, imaging spectrometer, and physically-based modeling for mapping snow water equivalent and snow albedo. Remote Sensing of Environment, 184, 139-152, 2016.

Penner, E.: Thermal conductivity of frozen soils. Canadian Journal of Earth Sciences, 7(3), 982-987, 1970.

Perron, C.J., Bennett, K., Lee, T.D.: Forest stewardship plan: Thompson farm. In: New Hampshire. Produced by Ossipee Mountain Land Company. University of West Ossipee, NH. https://colsa.unh.edu/sites/default/files/thompson-farm-plan.pdf, 2004.

Pflug, J. M., Fang, Y., Margulis, S. A., & Livneh, B.: Interactions between thresholds and spatial discretizations of snow: insights from estimates of wolverine denning habitat in the Colorado Rocky Mountains. Hydrology and Earth System Sciences, 27(14), 2747-2762, 2023.

Pflug, J. M., & Lundquist, J. D.: Inferring distributed snow depth by leveraging snow pattern repeatability: Investigation using 47 lidar observations in the Tuolumne watershed, Sierra Nevada, California. Water Resources Research, 56(9), e2020WR027243, 2020.

Pomeroy, J. W., & Brun, E.: Physical properties of snow. Snow ecology: An interdisciplinary examination of snow-covered ecosystems, 45, 118, 2001.

Proulx, H., Jacobs, J. M., Burakowski, E. A., Cho, E., Hunsaker, A. G., Sullivan, F. B., Palace, M., and Wagner, C.: Brief communication: Comparison of in situ ephemeral snow depth measurements over a mixed-use temperate forest landscape, The Cryosphere, 17, 3435–3442, https://doi.org/10.5194/tc-17-3435-2023, 2023.

Reinmann, A.B., Templer, P.H.: Increased soil respiration in response to experimentally reduced snow cover and increased soil freezing in a temperate deciduous forest. Biogeochemistry 140 (3), 359–371, 2018.

https://doi.org/10.5194/egusphere-2024-1530
Preprint. Discussion started: 21 June 2024

Revuelto, J., Alonso-Gonzalez, E., Vidaller-Gayan, I., Lacroix, E., Izagirre, E., Rodríguez-López, G., & López-Moreno, J. I.: Intercomparison of UAV platforms for mapping snow depth distribution in complex alpine terrain. Cold Regions Science and Technology, 190, 103344, 2021.

Schlögl, S., Lehning, M., & Mott, R.: How are turbulent sensible heat fluxes and snow melt rates affected by a changing snow cover fraction?. Frontiers in Earth Science, 6, 154, 2018.

Sorensen, P.O., Finzi, A.C., Giasson, M.A., Reinmann, A.B., Sanders-DeMott, R., Templer, P.H.: Winter soil freeze-thaw cycles lead to reductions in soil microbial biomass and activity not compensated for by soil warming. Soil Biol. Biochem. 116, 39–47, 2018.

Starks, P. J., Heathman, G. C., Jackson, T. J., & Cosh, M. H.: Temporal stability of soil moisture profile. Journal of hydrology, 324(1-4), 400-411, 2006.

Sturm, M., Goldstein, M.A., Parr, C.: Water and life from snow: A trillion dollar science question. Water Resour. Res. 53 (5), 3534–3544, 2017.

Stieglitz, M., Ducharne, A., Koster, R., Suarez, M.: The impact of detailed snow physics on the simulation of snow cover and subsurface thermodynamics at continental scales. J. Hydrometeorol. 2 (3), 228–242, 2001.

Trujillo, E., Ramírez, J.A., Elder, K.J.: Topographic, meteorologic, and canopy controls on the scaling characteristics of the spatial distribution of snow depth fields. Water Resour. Res. 43 (7) https://doi.org/10.1029/2006WR005317, 2007.

Tsang, L., Durand, M., Derksen, C., Barros, A. P., Kang, D. H., Lievens, H., et al.: Review article: Global monitoring of snow water equivalent using high-frequency radar remote sensing, The Cryosphere, 16, 3531–3573, https://doi.org/10.5194/tc-16-3531-2022, 2022.

Vachaud, G.A., Passerat de Silans, A., Balabanis, P., Vauclin, M.: Temporal stability of spatially measured soil water probability density function. Soil Sci. Soc. Am. J. 49, 822–828, http://dx.doi.org/10.2136/sssaj1985.03615995004900040006, 1985.

Vionnet, V., Brun, E., Morin, S., Boone, A., Faroux, S., Le Moigne, P., et al.: The detailed snowpack scheme Crocus and its implementation in SURFEX v7. 2. Geoscientific model development, 5(3), 773-791, 2012.

Wilson, G., Green, M., Brown, J., Campbell, J., Groffman, P., Durán, J., & Morse, J.: Snowpack affects soil microclimate throughout the year. Climatic change, 163, 705-722, 2020.

Yi, Y., Kimball, J. S., Rawlins, M. A., Moghaddam, M., & Euskirchen, E. S.: The role of snow cover affecting boreal-arctic soil freeze–thaw and carbon dynamics. Biogeosciences, 12(19), 5811-5829, 2015.

Zhang, T.: Influence of the seasonal snow cover on the ground thermal regime: An overview. Reviews of Geophysics, 43(4), 2005.